PROCEEDINGS OF SCIENCE

# Reconstruction and identification of hadronically decaying tau leptons with the ATLAS experiment

**Henrik Öhman**[*,†]
*Uppsala University*
*E-mail:* ohman@cern.ch

Tau leptons are important to many physical processes in high-energy physics. They are used for measurements of Standard Model processes, and searches for new physics beyond the Standard Model. With their high mass, tau leptons are prime signatures for e.g. Higgs boson decays to fermions. In these proceedings, the reconstruction and identification algorithms for hadronically decaying tau leptons in Run-2 of the LHC are presented, along with the identification performance in 13 TeV data collected in 2015.

*Fourth Annual Large Hadron Collider Physics*
*13-18 June 2016*
*Lund, Sweden*

*Speaker.
†on behalf of the ATLAS Collaboration



http://pos.sissa.it/

ATL-PHYS-PROC-2016-129
02/09/2016

PoS(LHCP2016)211

## 1. Introduction

Tau leptons ($\tau$) are the heaviest of the charged leptons, and the only leptons that can decay into hadrons (with a branching fraction of about 65 %). Their very short life time (0.3 ps) means that they typically decay before reaching the inner detector, and can only be identified via their decay products. The hadronic decays consist of an odd number of charged particles, and zero or more neutral particles, and a tau-type neutrino ($\nu_\tau$). Hadronic $\tau$ decays are used in searches for the Standard Model Higgs boson decays into $\tau^+\tau^-$ [1], for charged Higgs bosons in decays to $\tau\nu$ [2], and many other physics analyses in ATLAS.

## 2. Reconstruction

Jets with a transverse momentum $p_T > 10\,\mathrm{GeV}$ and pseudorapidity $|\eta| < 2.5$ are used to seed the $\tau$ reconstruction algorithm [3]. The *tau vertex* (TV) association algorithm finds the best match to the $\tau$ production among the primary vertex candidates. The TV defines the direction and coordinate system of the $\tau$ decay and ensures robustness against multiple $pp$ interactions (pile-up). Tracks from the inner detector are associated to $\tau$ decays in a small cone ($R < 0.2$) around its direction. The track selection is optimized to yield the largest efficiency for correctly reconstructing the number of charged hadrons (prongs) in simulated events. Figure 1 shows the efficiency for correct assignment of the $\tau$ production vertex, and the efficiency for reconstructing the correct number of associated tracks.

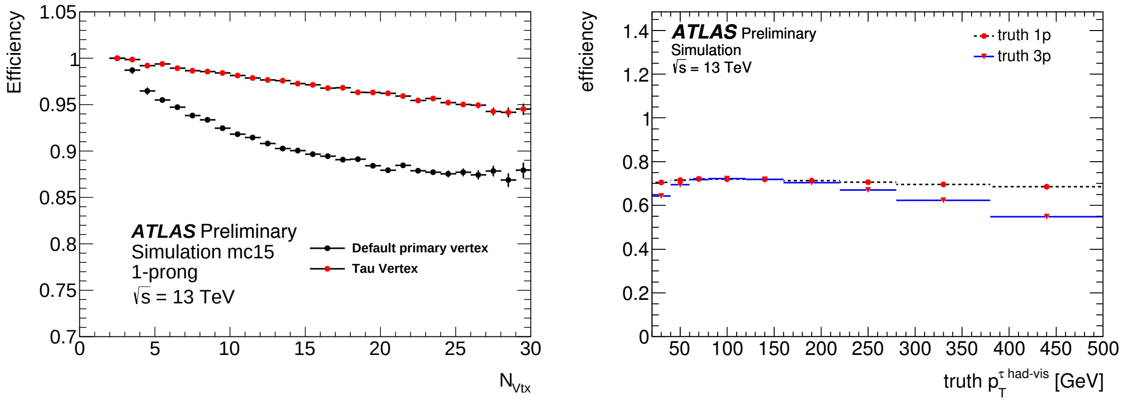


**Figure 1:** Efficiency for correct assignment of the $\tau$ production vertex for the TV association algorithm, as compared to the default primary vertex in the event, as a function of the number of primary vertices, for simulated 1-prong $\tau$ decays (left) [3]. Efficiency for reconstructing the correct number of associated tracks for simulated hadronic $\tau$ decays, as a function of the $p_T$ of the true visible decay products [3].

## 3. Jet discrimination

Hadronic $\tau$ decays are similar in appearance to jets from quarks or gluons, which are produced at a much higher rate. These jets are typically broader, and have different shapes as compared to hadronic $\tau$ decays. Jet rejection is performed with boosted decision tree (BDT) algorithms that use shower shape variables based on information about cells in the calorimeters and tracks in the inner detector. The variables include momentum of tracks and deposited energy in the calorimeters in the core ($\Delta R < 0.2$) and isolation ($0.2 < \Delta R < 0.4$) regions around the $\tau$ candidate direction, ratios of energy deposits from charged particles in the electromagnetic as compared to the hadronic calorimeter, information about the impact parameter (for 1-prong candidates) and secondary vertex (for 3-prong candidates), and the presence of neutral pions.

Compared to the identification algorithm in Run-1 [4], the input variables to the BDT algorithms are harmonized between the event reconstruction and the high-level trigger (HLT). The pile-up correction is based on the average number of interactions, instead of the number of primary vertices from the full reconstruction. The output from the $\pi^0$ reconstruction algorithm is replaced with some of its input variables. These changes result in equivalent levels of background rejection.

The BDT algorithms are trained using simulated $Z \to \tau\tau$ and multi-jet events. Three working points are defined, called *loose*, *medium*, and *tight*, corresponding to identification efficiencies of 0.6 (0.5), 0.55 (0.4), and 0.45 (0.3) respectively, for 1-prong (3-prong) $\tau$ decays. Figure 2 shows the identification efficiency, and the combined reconstruction and identification efficiency.

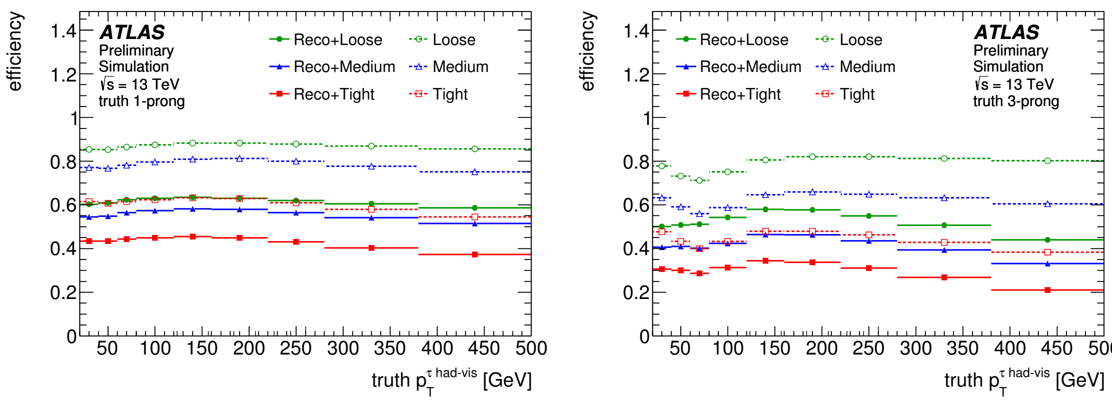


**Figure 2:** Efficiency for identification, and combined reconstruction and identification, for 1-prong (left) and 3-prong (right) simulated hadronic $\tau$ decays, as a function of the $p_{\mathrm{T}}$ of the true visible decay products [3].

## 4. Electron discrimination

The likelihood-based method [5] used to discriminate electrons against charged pions is also used to discriminate electrons against hadronic $\tau$ decays. The likelihood discriminator uses information about tracks from the inner detector, and about energy deposits in electromagnetic and hadronic calorimeters. Figure 3 shows the likelihood score distribution for hadronic $\tau$ decays and prompt electrons, and the background rejection power as a function of the $\tau$ identification efficiency. The nominal working point for the electron discrimination corresponds to a 95 % efficiency.

## 5. Energy scale

The $\tau$ energy scale (TES) consists of two corrections to the reconstructed energy. Contributions from pile-up interactions is subtracted, and a detector response function brings the energy

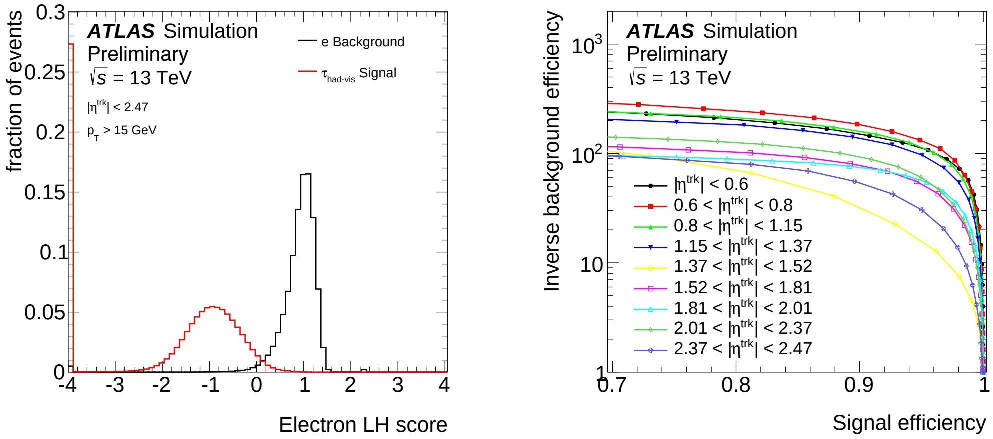


**Figure 3:** The electron likelihood score for 1-prong $\tau$ decays, as compared to electrons (left), and inverse background efficiency as a function of the $\tau$ identification efficiency in different regions of $|\eta|$ (right) [3]. Both the signal 1-prong hadronic $\tau$ decays, and the electron background are taken from simulated events.

to the scale of the true visible $\tau$ decay products. The pile-up correction increases linearly with the number of primary vertices. The detector response functions are derived with respect to pile-up corrected energy at the local hadronic (LC) scale [6]. Figure 4 shows the detector response function for 1- and multi-prong $\tau$ decays.

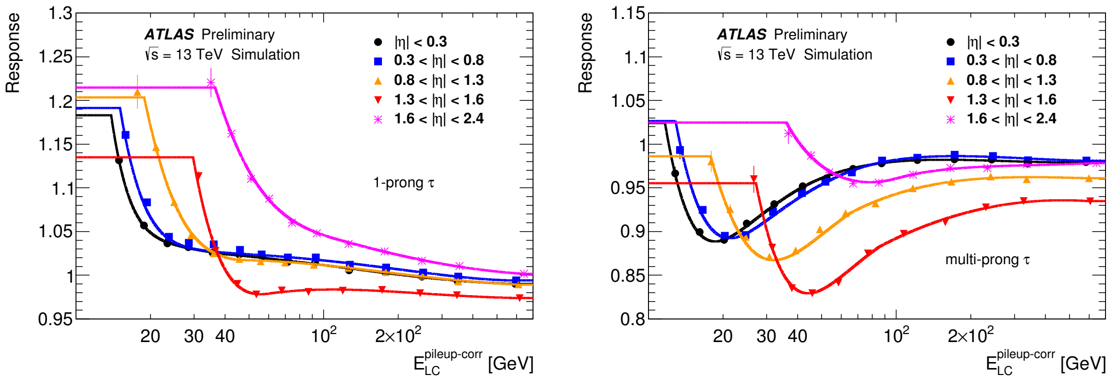


**Figure 4:** Detector response functions for 1- (left) and multi-prong (right) $\tau$ decays, in different regions in $|\eta|$ [3]. The distributions are fitted to an analytic function, and extrapolated to a constant for $\tau$ decay products with low transverse energy.

## 6. Performance measurements

The identification efficiency of hadronic $\tau$ decays is measured in data using a *tag-and-probe* analysis technique in $Z \to \tau\tau$ events, where one $\tau$ decays into a muon and the other hadronically. This selection allows the study of hadronic $\tau$ decays with high purity, and it is used to measure the identification efficiency both in the event reconstruction and the HLT. Figure 5 shows distributions of the BDT score in data compared to the expectation from simulated events and data-driven methods [7, 8].

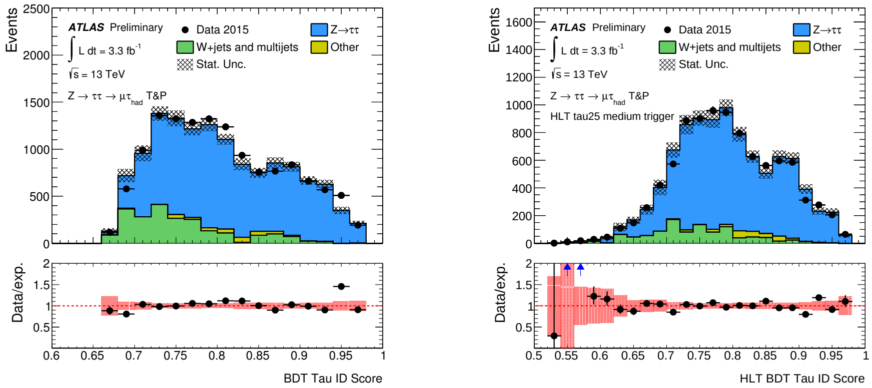


**Figure 5:** Distributions of the BDT score variable in the event reconstruction [7] (left) and the HLT [8] (right) measured in 13 TeV data collected in 2015, corresponding to an integrated luminosity of 3.3 $\text{fb}^{-1}$.

## 7. Conclusion

The reconstruction and identification algorithms for hadronically decaying tau leptons, as well as the hadronic $\tau$ energy scale calibration, are outlined. The differences in the identification algorithms between Run-1 and Run-2 are described. The *loose*, *medium*, and *tight* identification working points for jet discrimination correspond to efficiencies of 0.6 (0.5), 0.55 (0.4), and 0.45 (0.3) respectively, for 1-prong (3-prong) $\tau$ decays. The nominal working point for the electron discrimination corresponds to a 95 % $\tau$ identification efficiency. The identification performance in the event reconstruction and the HLT has been measured in 13 TeV data, and good agreement with simulated events and data-driven methods is observed.

## References

[1] ATLAS Collaboration, *Evidence for the Higgs-boson Yukawa coupling to tau leptons with the ATLAS detector*, JHEP 1504 (2015) 117, arXiv:1501.04943 [hep-ex].

[2] ATLAS Collaboration, *Search for charged Higgs bosons produced in association with a top quark and decaying via $H^{\pm} \to \tau\nu$ using pp collision data recorded at $\sqrt{s} = 13$ TeV by the ATLAS detector*, Phys.Lett. B759 (2016) 555-574, arXiv:1603.09203 [hep-ex].

[3] ATLAS Collaboration, *Reconstruction, Energy Calibration, and Identification of Hadronically Decaying Tau Leptons in the ATLAS Experiment for Run-2 of the LHC*, ATL-PHYS-PUB-2015-045, https://cds.cern.ch/record/2064383.

[4] ATLAS Collaboration, *Reconstruction of hadronic decay products of tau leptons with the ATLAS experiment*, Eur.Phys.J. C76 (2016) no.5, 295, arXiv:1512.05955 [hep-ex].

[5] ATLAS Collaboration, *Electron efficiency measurements with the ATLAS detector using the 2015 LHC proton-proton collision data*, ATLAS-CONF-2016-024, https://cds.cern.ch/record/2157687.

[6] ATLAS Collaboration, *Jet energy measurement with the ATLAS detector in proton-proton collisions at $\sqrt{s} = 7$ TeV*, Eur.Phys.J. C73 (2013) no.3, 2304, arXiv:1112.6426 [hep-ex].

[7] ATLAS Collaboration, https://twiki.cern.ch/twiki/bin/view/AtlasPublic/TauPublicCollisionPlots.

[8] ATLAS Collaboration, https://twiki.cern.ch/twiki/bin/view/AtlasPublic/TauTriggerPublicResults.